Available online at www.sciencedirect.com
SCIENCE DIRECT®
Journal of Power Sources 140 (2005) 157–161
JOURNAL OF POWER SOURCES
www.elsevier.com/locate/jpowsour

Short communication

Modeling capacity fade in lithium-ion cells

Bor Yann Liaw*, Rudolph G. Jungst, Ganesan Nagasubramanian, Herbert L. Case, Daniel H. Doughty

Sandia National Laboratories, Albuquerque, NM 87185, USA

Received 21 June 2004; accepted 13 August 2004

Abstract

Battery life is an important, yet technically challenging, issue for battery development and application. Adequately estimating battery life requires a significant amount of testing and modeling effort to validate the results. Integrated battery testing and modeling is quite feasible today to simulate battery performance, and therefore applicable to predict its life. A relatively simple equivalent-circuit model (ECM) is used in this work to show that such an integrated approach can actually lead to a high-fidelity simulation of a lithium-ion cell's performance and life. The methodology to model the cell's capacity fade during thermal aging is described to illustrate its applicability to battery calendar life prediction.

Keywords: Lithium-ion battery; Capacity fade; Equivalent-circuit model simulation; Battery life prediction; Thermal aging

1. Introduction

Accurate prediction of a battery's life, either the calendar or the cycle life, is a great technical challenge to any battery application. Battery life is an important issue for both traction and stationary applications because it is critically related to battery reliability and dependability, which in turn determines a power source's quality and eventual life-cycle cost. A battery's actual service life, however, depends on its history, during both the storage/standby and mission/duty periods experienced by the battery through its lifetime. Any sensible approach to predict battery life therefore has to address impacts from both the storage/standby and mission/duty periods.

In the past decade, due to substantial improvements in computer computation power and software capability, battery modeling and simulation [1–8] has enjoyed significant advancements. At the same time, experimental techniques that allow detailed investigation of interfacial and bulk properties of electrode materials have contributed to a better understanding of cell performance and degradation [9]. It is feasible to develop an integrated battery testing and simulation capability to assist battery R&D and operation [5,6].

There are a few attempts in the past to predict lithium-ion battery capacity. For example, Fuller et al. [10] used a 'first-principles' electrochemical model to estimate lithium-polymer cell capacity. Rakhmatov et al. [11] proposed an analytical model for lithium-ion cells used in portable electronic systems that can predict battery lifetime. Spotnitz [12] incorporated SEI growth into Fuller's model and began to look into the correlation of impedance change with capacity fade. Ramadass et al. [13] attempted to incorporate solvent reduction reaction into their first-principles electrochemical model to predict capacity fade.

We are much interested in taking a comprehensive, concurrent and hybrid approach [7,8] to develop tools and strategies that can predict the end-of-life (EOL) of a battery. Determination of the EOL of a battery system in service is very difficult, expensive, and often destructive to the system. Therefore, non-invasive, non-destructive techniques that can determine

* Corresponding author. Tel.: +1 808 956 2339; fax: +1 808 956 2336.
E-mail address: bliaw@hawaii.edu (B.Y. Liaw).

0378-7753/$ – see front matter © 2004 Elsevier B.V. All rights reserved.
doi:10.1016/j.jpowsour.2004.08.017

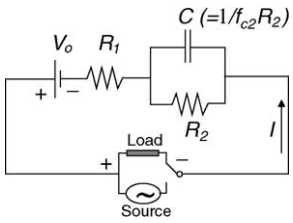

Fig. 1. The ECM used in this work.

the EOL without removing the system from service are highly desired.

Sandia has been involved in studying the performance of a group of 18650-size lithium-ion batteries (LIB) that was fabricated for the US Department of Energy (USDOE) Advanced Technology Development (ATD) Program. These batteries contain a high-power chemistry [9,14–16]. One of the objectives of the ATD Program is to develop procedures to make rapid comparisons of performance–degradation rates and predictions of battery life. This paper will discuss a simple LIB modeling approach that uses an equivalent-circuit model (ECM) to simulate cell performance, particularly the capacity fade phenomenon. This example shows that we can simulate battery performance changes due to thermal aging, which is one of the most influential factors impacting battery calendar life during storage, standby or operation periods.

2. The equivalent-circuit model (ECM)

There are several ECM approaches of different nature and flavor reported by others (e.g., [17–19]) for simulating LIB performance. A schematic of the ECM used in this work is shown in Fig. 1. The model resembles to that used by Verbrugge and Conell [19] for Ni-MH cells. We favor this model due to its simplicity, yet flexibility, in describing an electrochemical system via the separation of all ohmic resistance components from all faradic non-linear components, as they are lumped into R_1 and R_2C, respectively. This generic nature makes this ECM applicable to a variety of chemistries (e.g., valve-regulated lead acid [7], Ni-MH [19], or LIB in this paper).

To construct a valid model, we first need to incorporate the state-of-charge (SOC)-dependent open circuit voltage (OCV) and resistance (R_1 and R_2) values into the model. Fig. 2 shows these SOC-dependent values for the chemistry used in this work. The OCV values were determined from a cell discharged at $C/25$ rate, as reported in [20]. The resistance versus SOC relationship can be derived from two sources of experimental data, either from ac impedance measurements or from the galvanostatic dc polarization, which yields discharge curves at different rates. A more detailed discussion of how the values were derived can be found in [8]. We should note that in the model, the resistance R_2 was assumed to consist of two independent contributions, R_2' and R_2'', as shown in Fig. 2, to approximate the resistance change with SOC. The

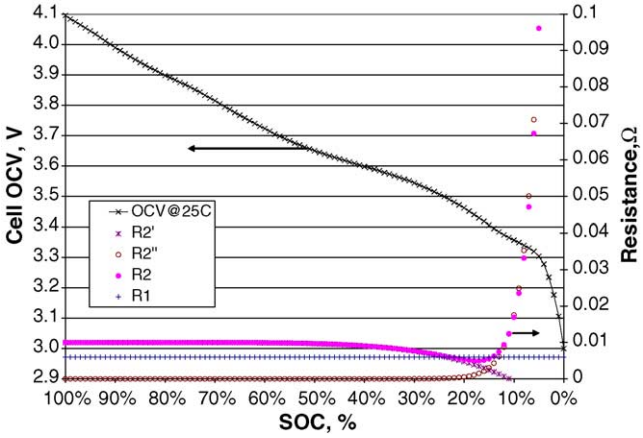

Fig. 2. SOC-dependent OCV and resistance values used in ECM.

function of R_2' follows a power law with SOC, while that of R_2'' is an exponential function with SOC, as shown in Eqs. (1) and (2).

$$R_2' = a + b(\mathrm{SOC})^c \tag{1}$$

$$R_2'' = d\exp[(1-\mathrm{SOC})e] \tag{2}$$

Thus,

$$R_2 = a + b(\mathrm{SOC})^c + d\exp[(1-\mathrm{SOC})e] \tag{3}$$

These functions are empirical and do not imply any physical meaning in this work, although further analysis of their dependence with aging time and conditions could provide us some clues as to what process might be shaping the physical change of the cell performance. This would need to be verified by additional experimental evidence. The capacitance value, C, can be derived from the characteristic frequency, $f_{c2} = 1/R_2C$, which is yielded from the Nyquist plot of the cell as demonstrated in Fig. 3. The time-dependent cell voltage discharge curve can then be calculated from the ECM for a constant-current condition [19], according to Eq. (4):

$$V(t) = \frac{Q(0)}{C}\mathrm{e}^{-t/R_2C} + V_\mathrm{o} - IR_1 - IR_2(1-\mathrm{e}^{-t/R_2C}) \tag{4}$$

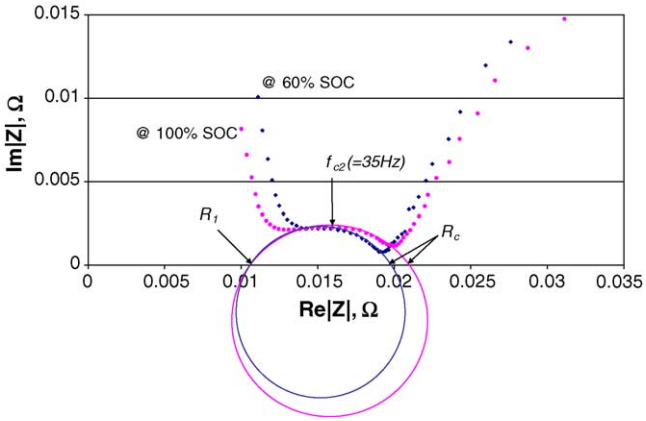

Fig. 3. Nyquist plot for cell #319 measured at 60% and 100% SOC.

where I is constant, $Q(0)$ is the nominal capacity, and V_o the nominal SOC-dependent cell OCV. Thus, for any given time step, the charge passed is calculated to derive the SOC value at the end of the step, and the associated OCV and resistance values are plugged into Eq. (4) to give the cell voltage as a function of time.

3. Experimental

Quallion LLC (Sylmar, CA) provided test cells as part of the USDOE ATD Program efforts, and Sandia along with four other National Labs was commissioned to evaluate the cell performance for hybrid electric vehicle applications. Detailed descriptions of the chemistry, cell configuration, test protocols and procedures, and test results can be found in [9,16,20]. In short, this high-power cell chemistry uses a cathode consisting of $LiNi_{0.8}Co_{0.15}Al_{0.05}O_2$, an anode fabricated with MAG-10 graphite, and an electrolyte consisting of ethylene carbonate (EC)/ethyl methyl carbonate (EMC) (3:7 wt.% ratio) with 1.2 M $LiPF_6$.

The data used in this paper were extracted from that obtained for a cell (#319) in the pool of Sandia's test cells as an example. This particular cell went through thermal aging at 55 °C and 100% SOC for about 20 weeks, while the other lithium-ion cells were aged at temperatures ranging from 25 °C to 55 °C and at 60%, 80%, or 100% SOC to examine the cell's power and capacity degradation. Cell #319 was chosen because its behavior is representative of the group of cells that went through the same thermal-aging conditions.

The cell performance as received and during subsequent tests at four-week intervals was evaluated by a reference performance test (RPT), as described in [20]. The cell capacity was determined at $C/1$ and $C/25$ discharge rates in RPTs after each thermal-aging period. ac impedance data were also collected, and were intended to identify which cell components were changing in the aging process. Other National Laboratories on the ATD Program are conducting more detailed diagnostic analyses to understand the degradation mechanism. The discharge curves from the discharge regimes at $C/25$ and $C/1$ and the ac complex impedance data generated in the RPTs were used in deriving the parameters for model development and validation.

4. Results and discussion

Fig. 4 shows a series of discharge curves at various rates, from $C/25$ to $10C$, simulated by the ECM using Eq. (4). Also shown are two sets of experimental data obtained at $C/25$ and $C/1$ rate. The very high degree of agreement between the actual data and the simulated results gives us a high level of confidence about the resistance values that we used in the model. It is worth mentioning that the fit of the parameters is also demonstrated by the ability to capture the essence of

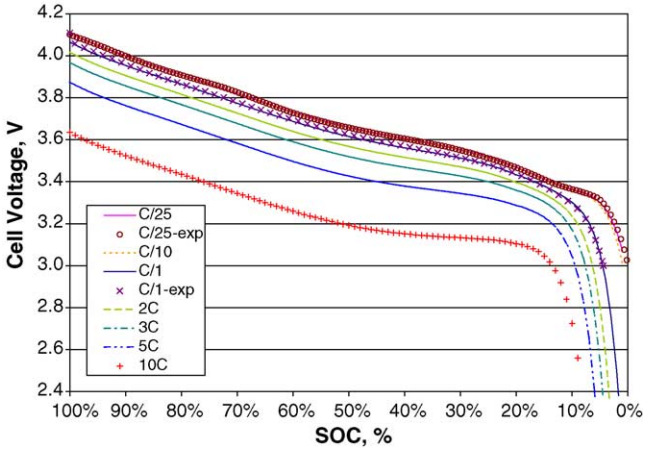

Fig. 4. Discharge curves simulated by ECM using Eq. (4) and the data obtained at $C/25$ and $C/1$ for comparison and validation.

the shape of the discharge curves. This is achieved primarily by the use of the two contributions, R_2' and R_2'', in R_2. The more consistency achieved, the better we can distinguish any subtle differences from the parameters used to interpret the results. Eventually, this capability can be used to analyze subtle differences from various phenomenological assumptions and the corresponding reflection in the parameters applied to the battery's physical model to help us study the impacts on the power-delivery capability, capacity, and life.

The ability to simulate cell voltage under galvanostatic charge or discharge regimes is quite useful for battery R&D. For example, by imposing a suitable cut-off condition, we can calculate the amount of charge put in and released from the cell to yield the rate capacity, as well as charge efficiency. Furthermore, if the aging effects and degradation rates are known, we can perform simulations using various temperature and power conditions imposed onto the cell to simulate the life performance.

In order to simulate the capacity fade of the cell, we need to know how cell characteristics such as OCV and resistance values change with aging time and conditions. Since OCV and R_1 are intrinsic to the cell, their changes under thermal aging should be negligible. Therefore, we treated them as invariant in this work. $R_1 = 0.011\ \Omega$ was used throughout the work, independent of SOC and aging conditions.

The only characteristic that requires attention is the change in R_2. Fig. 5 shows how the five parameters in Eq. (3) change with the aging period under the same aging condition. These relationships allow us to interpolate or extrapolate parameter values over a specific aging period to permit prediction of the cell performance characteristics under the aging condition. Parameter a is a constant and independent of SOC, and parameters b and c change in linear fashions. Parameter d, the pre-exponential factor, changes in a 3rd order polynomial while e changes in a power law fashion.

Fig. 6 shows total cell resistance from the above five parameters in Eq. (3) and R_1. The overall resistance of the cell

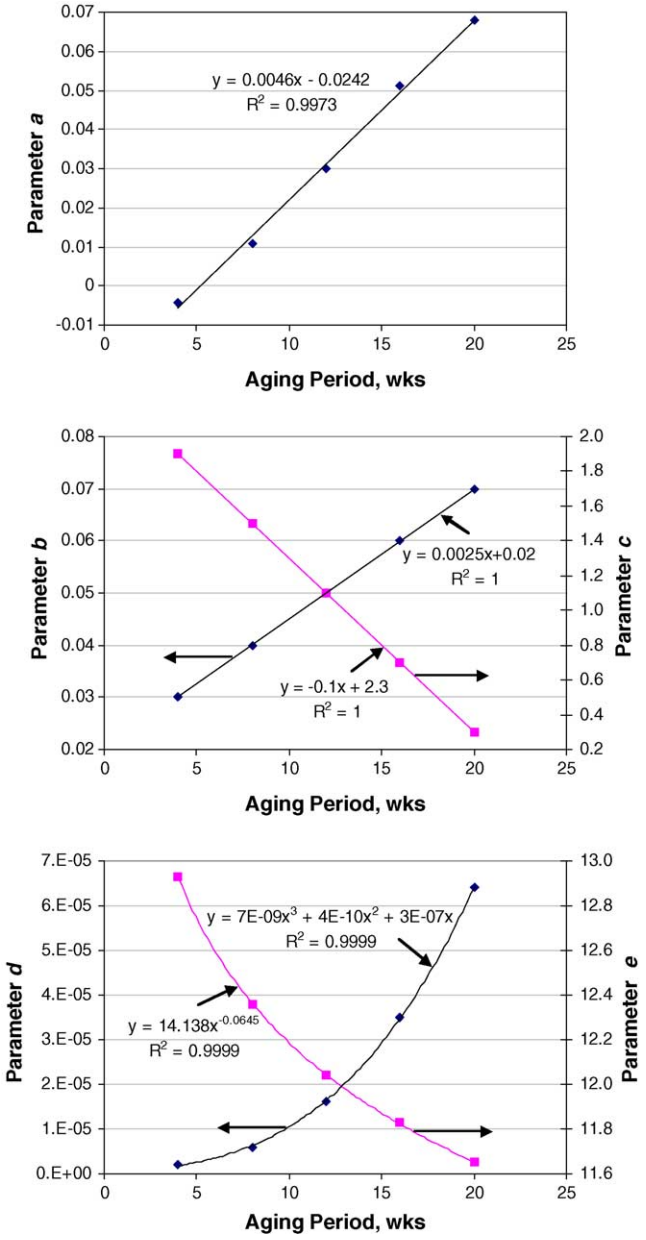

Fig. 5. Trends of parameters a to e in Eq. (3) versus aging period.

as a function of SOC increases as the cell ages. We also notice that although the resistance increases occurred across the entire SOC range, they are more noticeable in the lower SOC region, thus leading to a higher rate of capacity fade. The separation of R_2 into two independent contributions of R_2' and R_2'' allows a disproportional rate of increase in R_2' and R_2'', making the approach more suitable and easier to reflect characteristic changes in capacity fade.

Fig. 7 shows the results of using this set of parameters in ECM to simulate the discharge behavior of the cell going through the thermal-aging experiments. The five discharge curves simulated from the ECM are consistent with the experimental data. The differences between the predicted capacity and the experimental data are compared in Fig. 8.

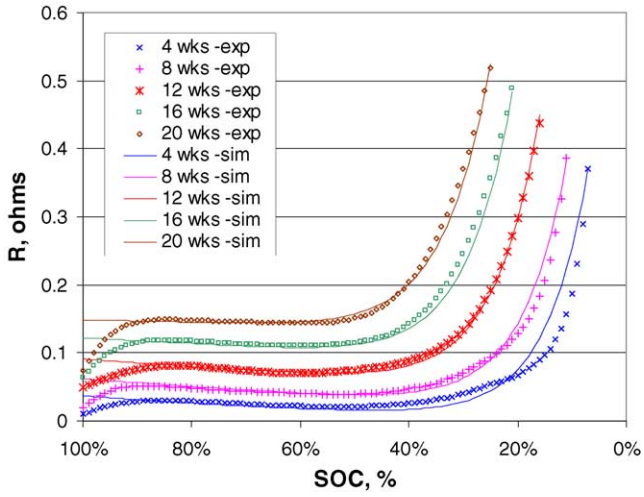

Fig. 6. Characteristics of resistance change versus SOC as the cell goes through the thermal aging. Symbols are experimental data. Lines are values estimated from Eq. (3) with parameters in Fig. 5 and R_1.

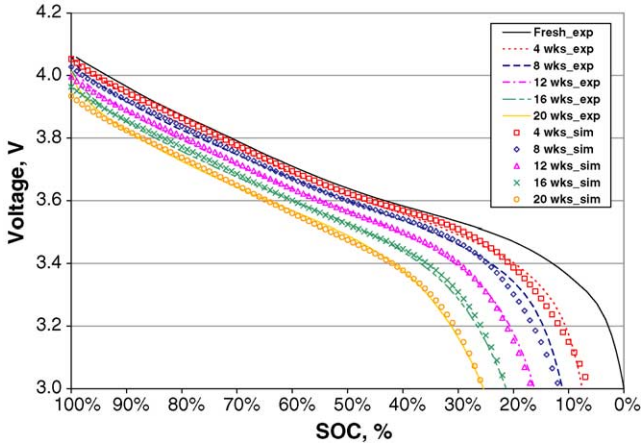

Fig. 7. Simulated discharge curves (symbols) with two independent contributions in R_2 in the ECM, in comparison with the experimental results (lines).

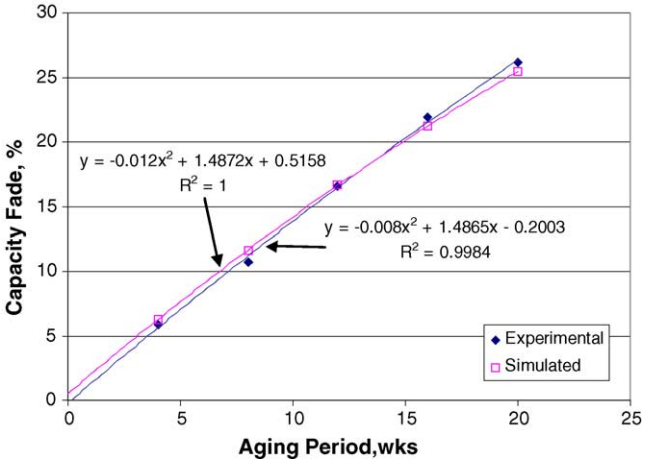

Fig. 8. Comparison of capacity fade measured from experiments and simulated from ECM. Polynomial fitting allows projection of battery calendar life under the thermal-aging condition.

The introduction of the two resistance contributions in R_2, one that follows a power law dependence with SOC, and the other exponential is somehow essential in order to properly simulate the discharge behavior, and thus the capacity change induced by the thermal-aging process. Although not specifically illustrated, we have also tried to treat the resistance R_2 with a single expression of polynomial fitting. This treatment, however, would not lead to a disproportional increase in resistance at different regions of the SOC. Thus, the profound capacity fade in the lower SOC region could not be captured with this particular approach using a consistent set of parameterization. In other words, unlike the clear relationships displayed in Fig. 5, we might, at best, generate each curve under degradation with an isolated set of purely empirical parameters, such that it bears no analytical meaning at all. Therefore, the introduction of the two resistance contributions in R_2 not only allows us to assign an asymmetric dependence of R_2 with SOC but also enables us to retain a consistent trend of parameterization for capacity fade prediction.

From the parameterization shown in Fig. 5, we would further like to point out that

(i) The $a + b(\mathrm{SOC})^c$ term in Eq. (1) did change with thermal aging and induced an increase in polarization resistance that undermined the cell capacity. However, this increase only attributed to the capacity loss in the high SOC region. It did not affect the capacity fade in a predominant manner since the capacity fade primarily came from the capacity loss in the low SOC region.

(ii) The capacity fade is primarily governed by the term $d\exp[(1-\mathrm{SOC})e]$ in Eq. (2), and profoundly following the rapid increase in the pre-exponential factor, d.

(iii) Finally, Fig. 8 shows the model prediction and actual experimental data, in which the capacity fade projection and measurement are compared. The polynomial fittings will allow the prediction of battery calendar life under this particular thermal-aging process, once the EOL condition is defined.

5. Conclusion

We have demonstrated that high-fidelity simulation of battery performance and capacity fade can be achieved with a simple equivalent-circuit model using a consistent set of parameters that reflect thermal aging. This high-performance simulation can assist us to predict the battery life under thermal-aging conditions, which are the most critical factors in determining the battery calendar life. With increasing accuracy in predicting the battery performance and degradation, we can use this approach to understand the trend of resistance change during thermal aging and the impact from such a change on battery performance and life.

Acknowledgments

Sandia National Laboratories is a multi-program laboratory operated by Sandia Corporation, a Lockheed-Martin Company, for the United States Department of Energy's National Nuclear Security Administration under Contract DE-ac04-94AL85000. The USDOE FreedomCAR and Vehicle Technology Office through the ATD High-Power Battery Program funded the lithium-ion battery testing and data collection. The battery-life prediction modeling was funded by USDOE under the Energy Storage Program.

References

[1] J. Newman, Electrochemical Systems, second ed., Prentice Hall, Englewood Cliff, NJ, 1991.
[2] C.Y. Wang, W.B. Gu, B.Y. Liaw, J. Electrochem. Soc. 145 (1998) 3407.
[3] W.B. Gu, C.Y. Wang, B.Y. Liaw, J. Electrochem. Soc. 145 (1998) 3418.
[4] B. Wu, M. Mohammed, D. Brigham, R. Elder, R.E. White, J. Power Sources 101 (2001) 149.
[5] B.Y. Liaw, K.P. Bethune, X.G. Yang, J. Power Sources 110 (2002) 330.
[6] B.Y. Liaw, X.G. Yang, K.P. Bethune, Solid State Ionics 152/153 (2002) 51.
[7] B.Y. Liaw, Presented in the Joint Meeting of International Battery Association and the Fifth Hawaii Battery Conference 2003, Waikoloa, Hawaii, January 7–10, 2003.
[8] B.Y. Liaw, G. Nagasubramanian, R.G. Jungst, D.H. Doughty, Presented in the 14th International Conference on Solid State Ionics, Monterey, CA, June 22–27, 2003 (to be published in Solid State Ionics).
[9] FY2001 Annual Progress Report for the ATD Program, US Department of Energy, Office of Transportation Technologies, available at <http://www.cartech.doe.gov/pdfs/B/196.pdf>.
[10] T.F. Fuller, M. Doyle, J. Newman, J. Electrochem. Soc. 141 (1994) 1;
T.F. Fuller, M. Doyle, J. Newman, J. Electrochem. Soc. 141 (1994) 982.
[11] D. Rakhmatov, S. Vrudhula, Proceedings of the International Conference on Computer Aided Design, ICCAD'01 (2001);
D. Rakhmatov, S. Vrudhula, D. Wallach, Proceedings of the International Symposium on Low Power Electronics and Design, ISLPED'02 (2002).
[12] R. Spotnitz, J. Power Sources 113 (2003) 72.
[13] P. Ramadass, et al., J. Electrochem. Soc. 151 (2004) A196.
[14] R. G. Jungst, D. H. Doughty, B. Y. Liaw, G. Nagasubramanian, H. L. Case, E. V. Thomas, Proceedings of the 40th Power Sources Conference, Cherry Hill, NJ, June 2002.
[15] R.G. Jungst, G. Nagasubramanian, H.L. Case, B.Y. Liaw, A. Urbina, T.L. Paez, D.H. Doughty, J. Power Sources 119–121 (2003) 870.
[16] B.Y. Liaw, E.P. Roth, R.G. Jungst, G. Nagasubramanian, H.L. Case, D.H. Doughty, J. Power Sources 119–121 (2003) 874.
[17] E. Barsoukov, J.H. Kim, C.O. Yoon, H. Lee, J. Power Sources 83 (1999) 61.
[18] E. Karden, S. Buller, R.W. De Doncker, Electrochim. Acta 47 (2002) 2347.
[19] M.W. Verbrugge, R.S. Conell, J. Electrochem. Soc. 149 (2002) A45.
[20] PNGV Test Plan for Advanced Technology Development Gen 2 Lithium-Ion Cells, EHV-TP-121, Revisions 1 through 6, US Department of Energy, Office of Transportation Technologies, 2002.